Published in final edited form as:
Bioorg Med Chem Lett. 2012 March 1; 22(5): 1985–1988. doi:10.1016/j.bmcl.2012.01.029.

Structure-activity relationship study of selective benzimidazole-based inhibitors of *Cryptosporidium parvum* IMPDH

Sivapriya Kirubakaran[a,1], **Suresh Kumar Gorla**[a], **Lisa Sharling**[b], **Minjia Zhang**[a], **Xiaoping Liu**[b], **Soumya S. Ray**[d], **Iain S. MacPherson**[a], **Boris Striepen**[b,c], **Lizbeth Hedstrom**[a,e], and **Gregory D. Cuny**[f,*]

[a]Department of Biology Brandeis University, MS009, 415 South Street, Waltham, MA 02454

[b]Center for Tropical and Emerging Global Diseases University of Georgia, 500 D.W. Brooks Drive, Athens, GA, 30602

[c]Department of Cellular Biology, University of Georgia, 500 D.W. Brooks Drive, Athens, GA, 30602

[d]Center for Neurologic Diseases, Department of Neurology, Brigham & Women's Hospital and Harvard Medical School, 65 Landsdowne Street, Cambridge, MA 02139

[e]Department of Chemistry, Brandeis University, MS009, 415 South Street, Waltham, MA 02454

[f]Laboratory for Drug Discovery in Neurodegeneration, Brigham & Women's Hospital and Harvard Medical School, 65 Landsdowne Street, Cambridge, MA 02139

Abstract

Cryptosporidium parasites are important waterborne pathogens of both humans and animals. The *C. parvum* and *C. hominis* genomes indicate that the only route to guanine nucleotides is via inosine 5'-monophosphate dehydrogenase (IMPDH). Thus the inhibition of the parasite IMPDH presents a potential strategy for treating *Cryptosporidium* infections. A selective benzimidazole-based inhibitor of *C. parvum* IMPDH (*Cp*IMPDH) was previously identified in a high throughput screen. Here we report a structure-activity relationship study of benzimidazole-based compounds that resulted in potent and selective inhibitors of *Cp*IMPDH. Several compounds display potent antiparasitic activity *in vitro*.

Cryptosporidiosis is a waterborne diarrheal disease caused by protozoan parasites of the genus *Cryptosporidium*[1, 2]. While *Cryptosporidium hominis* is specific to humans, others such as *C. parvum* infect humans and a wide range of animals and can be transmitted zoonotically. Cryptosporidiosis is a major cause of malnutrition in the developing world and can be life threatening in immunocompromised patients. *Cryptosporium* oocysts are resistant to commonly employed methods of water treatment, leading to frequent outbreaks in the developed world. In addition, oocysts are relatively easy to obtain, and therefore pose a credible biowarfare threat. No vaccines exist for *Cryptosporidium* infections and the

*Corresponding author. hedstrom@brandeis.edu; *phone: 781-736-2333; fax: 781-736-2349*.
[1]Present address: Dana-Farber Cancer Institute, Department of Biological Chemistry and Molecular Pharmacology Harvard Medical School, Seeley G. Mudd building, Room 628, 250 Longwood Ave. Boston, MA 02115

approved drugs are not particularly effective. Therefore, the tools currently available to combat a massive outbreak are limited.

Like other apicomplexan parasites, *Cryptosporidium* is unable to synthesize purine nucleotides *de novo*. Instead, *Cryptosporidium* relies on a highly streamlined purine salvage pathway[3–5]. The parasite obtains adenosine from the host, which is converted sequentially to AMP and IMP. The enzyme inosine 5'-monophosphate dehydrogenase (IMPDH) converts IMP to XMP (Scheme 1). XMP is subsequently converted to GMP. *Cryptosporidium* does not contain guanine salvage enzymes, so this pathway appears to be the only route to guanine nucleotides.

Interestingly, *Cryptosporidium* acquired its IMPDH gene by lateral gene transfer from an ε-proteobacterium and consequently the enzyme is highly divergent from the host counterpart[6]. Thus, selective inhibition of *Cryptosporidium* IMPDH presents a potential strategy for treating cryptosporidiosis with minimal effects on its mammalian host[7–9]. The benzimidazole analog **C** was identified in a high throughput screen targeting the highly diverged NAD binding site of *C. parvum* IMPDH (*Cp*IMPDH; this protein is identical to *C. hominis* IMPDH) (Figure 1).[7] Compound **C** is a moderately potent but highly selective inhibitor for *Cp*IMPDH (IC_{50} = 1.2 μM) with no detectable activity against the human IMPDH1 and IMPDH2 (IC_{50} > 50 μM).

The structure of *Cp*IMPDH in complex with IMP and the **C** derivative **C64** was recently solved[10]. This structure revealed the presence of a cavity next to the aniline ring of **C64**, suggesting that more potent inhibitors would be obtained if the 4-bromoaniline group was replaced with bulkier groups. This information was used to guide the design of **C90** and **C97**[10]. As expected, the substitution of 2-naphthyl for the 4-bromoaniline increased potency, with **C90** and **C97** exhibiting values of IC_{50} of 7–8 nM (Table 1). Herein, we report a more comprehensive structure-activity relationship (SAR) study for this class of inhibitors.

The benzimidazole analogs were synthesized following the procedure outlined in Scheme 2. Various acetylamide derivatives **3** were prepared by treating substituted anilines **1** with bromo acetylchlorides, **2**, in dichloromethane (DCM) and in the presence of catalytic amounts of 4-N, N-dimethylaminopyridine (DMAP). Various 2-substituted benzimidazoles **6** were prepared by condensing o-phenylene diamine **4** with aromatic aldehydes followed by oxidation in the presence of sodium metabisulfite using a slight modification of published procedures[11]. Finally, 2-substituted benzimidazoles were coupled with the acetylamides **3** in the presence of potassium carbonate to yield benzimidazoles **7**. *Cp*IMPDH inhibiton was measured by monitoring the production of NADH in the presence of varying inhibitor concentrations[9]. Inhibition was also determined in the presence of 0.05% fatty acid free bovine serum albumin (BSA) in order to evaluate the effects of non-specific binding. Gratifyingly, none of the *Cp*IMPDH inhibitors displayed activity against human IMPDH2 (IC_{50} > 5 μM). Selected compounds were also evaluated for antiparasitic activity[12].

The first region of the molecule examined was the anilide substituent. Replacing the 4-methoxy of **C** with a thiomethyl (**C39**) resulted in a ten-fold increase in activity (Table 1). However, a branched aliphatic group (**C43**) at the same position resulted in decreased activity. Interestingly, replacing the 4-methoxy with electron withdrawing groups (**C9** – **C11**, **C58**, **C14**, **C45**) resulted in compounds with increased activity, except for sulfone **C40**. Larger more hydrophobic groups such as chlorine (**C10**) and bromine (**C14**) were best. Translocation of the chlorine from the 4-position to either the 3- or 2- positions (**C20**, **C48**) was detrimental. Several compounds containing electron withdrawing groups in the 3- and 4-positions (**C86** and **C93**) also demonstrated potent inhibitory activity. Surprisingly,

addition of a chlorine to the 2-naphthyl (**C28**) was not tolerated. Introduction of a methyl onto the methylene between the amide carbonyl and the imidazole resulted in increased potency in one case (**C79** vs. **C10**), but decreased activity in another case (**C87** vs. **C86**). Increasing the steric bulk of the methyl group to i-Pr (**C24**) was detrimental. Finally, inserting a methylene between the amide NH and the phenyl ring (**C18**) was not tolerated.

Subsequently, the SAR of the 4-thiazolyl ring was examined (Table 2). As reported previously, changing the connectivity to a 2-thiazolyl increased activity for several analogs (**C61** vs. **C10**, **C64** vs. **C14**, **C74** vs. **C79**) and retained potent activity for another analog (**C97** vs. **C90**)[10]. The 5-thiazolyl was also comparatively active (**C67** vs. **C61**). In addition, several other heterocycles (**C62, C100**, **C16**) also retained potent activity. However, the 2-pyrrolyl (**C65**) and 2-oxazolyl (**C69**) derivatives demonstrated reduced potency. Likewise, replacing the thiazole ring by various phenyls (**C17**, **C31**, **C59**) or a methyl (**C38**) resulted in significant losses in activity.

In order to further analyze the SAR results, select molecules were docked using GLIDE (Schrödinger Inc.) into a *Cp*IMPDH model based on the previously determined co-crystal structure. Free energy perturbation (FEP) calculations were then determined (calculated as ΔΔG relative to inhibitor **C**) and the results were highly correlated ($r^2 = 0.93$) to the observed IC_{50} determinations (Table 3, Figure 2)[13]. Inhibitor potency appears to be driven largely by two major contributions: (1) a hydrogen bond between E329 of *Cp*IMPDH and the amide NH of the inhibitors; (2) an entropic effect of displacing water molecules from the binding cavity by large hydrophobic substituents. The presence of strong electron withdrawing groups on the arylamide increases potency by increasing the strength of the E329-NH H-bond provided no steric clashes are present. Thus the balance between conformational state and electron withdrawing ability appears critical for determining the final potency of the inhibitors. For example, 3,4-dichloro substituted analog **C86** is predicted to be more potent than the 3-chloro analog **C48**. For the 2-chloro analog **C20** a steric clash is predicted to change the orientation of the phenyl ring lowering the inductive effect of the chlorine substituent weakening the E329-NH bond. For the 2-naphthyl analog **C90**, displacement of ordered water molecules from the active site of the protein is entropically favored resulting in ΔΔG relative to **C** of −5.87 kcal/mol and an IC_{50} value of 7 nM.

Compounds with a value of IC_{50} less than 30 nM were candidates for testing in a *Toxoplasma gondii* model of *C. parvum* infection[12]. Preference was given to compounds that displayed little non-specific binding as judged by changes in the value of IC_{50} in the presence of BSA. Wild type *T. gondii* expresses a eukaryotic IMPDH that is resistant to the *Cp*IMPDH inhibitors. In contrast, in the *T. gondii*/*Cp*IMPDH model parasite, the endogenous IMPDH gene has been replaced with *Cp*IMPDH. In addition, the gene encoding hypoxanthine-guanine-xanthine phosphoribosyltransferase was knocked out, so this strain relies on the activity of *Cp*IMPDH to obtain guanine nucleotides. Both *T. gondii* strains express yellow fluorescent protein enabling easy monitoring of parasite proliferation. *T. gondii* strains were cultured in human foreskin fibroblasts immortalized with hTERT, so this assay also reports on host cell toxicity. Compounds **C64**, **C84**, **C90**, **C91** and **C97** all displayed sub-micromolar activity against *T. gondii*/*Cp*IMPDH (Table 4). **C64** and **C97** displayed selectivity • 30 versus the wild-type strain, strongly indicating that antiparasitic activity results from the inhibition of *Cp*IMPDH.

Compounds **C64**, **C84**, **C90** and **C97** were also tested in an *in vitro* model of *C. parvum* infection[12]. Importantly, all four compounds are approximately two orders of magnitude more potent than paromomycin, the standard control for anticryptosporidial activity (literature paromomycin EC_{50} values are 65–130 μM[7, 12, 14–16]). The potencies of **C64**, **C84**, **C90** and **C97** were similar to that observed in the *T. gondii* model (Table 4).

In conclusion, a SAR study of benzimidazole-based *Cp*IMPDH inhibitors revealed that variations to the aniline and to the heterocycle attached to the 2-position of the benzimidazole could be altered in order to increase inhibitory activity, while retaining excellent selectivity over human IMPDH2. The benzimidazole-based *Cp*IMPDH inhibitors described herein could serve as useful molecular probes for studying *C. parvum* and other related organisms in addition to providing lead compounds for the development of effective treatments of cryptosporidiosis.

Supplementary Material

Refer to Web version on PubMed Central for supplementary material.

Acknowledgments

This work was supported by funding from the National Institute of Allergy and Infectious Diseases (U01AI075466) to LH. GDC thanks the New England Regional Center of Excellence for Biodefense and Emerging Infectious Diseases (NERCE/BEID), and the Harvard NeuroDiscovery Center for financial support. BS is a Georgia Research Alliance Distinguished Inverstigator. IC_{50} data for these compounds are maintained using ChemAxon, http://www.chemaxon.com/.

References and notes

1. Fayer R. Vet Parasitol. 2004; 126:37. [PubMed: 15567578]
2. Huang DB, White AC. Gastroenterol Clin North Am. 2006; 35:291. [PubMed: 16880067]
3. Abrahamsen MS, Templeton TJ, Enomoto S, Abrahante JE, Zhu G, Lancto CA, Deng M, Liu C, Widmer G, Tzipori S, Buck GA, Xu P, Bankier AT, Dear PH, Konfortov BA, Spriggs HF, Iyer L, Anantharaman V, Aravind L, Kapur V. Science. 2004; 304:441. [PubMed: 15044751]
4. Xu P, Widmer G, Wang Y, Ozaki LS, Alves JM, Serrano MG, Puiu D, Manque P, Akiyoshi D, Mackey AJ, Pearson WR, Dear PH, Bankier AT, Peterson DL, Abrahamsen MS, Kapur V, Tzipori S, Buck GA. Nature. 2004; 431:1107. [PubMed: 15510150]
5. Striepen B, Pruijssers AJ, Huang J, Li C, Gubbels MJ, Umejiego NN, Hedstrom L, Kissinger JC. Proc Natl Acad Sci U S A. 2004; 101:3154. [PubMed: 14973196]
6. Striepen B, White MW, Li C, Guerini MN, Malik SB, Logsdon JM Jr. Liu C, Abrahamsen MS. Proc Natl Acad Sci U S A. 2002; 99:6304. [PubMed: 11959921]
7. Umejiego NN, Gollapalli D, Sharling L, Volftsun A, Lu J, Benjamin NN, Stroupe AH, Riera TV, Striepen B, Hedstrom L. Chem Biol. 2008; 15:70. [PubMed: 18215774]
8. Umejiego NN, Li C, Riera T, Hedstrom L, Striepen B. J Biol Chem. 2004; 279:40320. [PubMed: 15269207]
9. Maurya SK, Gollapalli DR, Kirubakaran S, Zhang M, Johnson CR, Benjamin NN, Hedstrom L, Cuny GD. J Med Chem. 2009; 52:4623. [PubMed: 19624136]
10. MacPherson IS, Kirubakaran S, Gorla SK, Riera TV, D'Aquino JA, Zhang M, Cuny GD, Hedstrom L. J Am Chem Soc. 2010; 132:1230. [PubMed: 20052976]
11. Yang D, Fokas D, Li J, Yu L, Baldino CM. Synthesis. 2005:47.
12. Sharling L, Liu X, Gollapalli DR, Maurya SK, Hedstrom L, Striepen B. PLoS Negl Trop Dis. 2010; 4:e794. [PubMed: 20706578]
13. Protein data base (PDB) file 3KHJ was used to generate a model for the protein bearing the missing side chains, loops and hydrogen atoms. The loop positions were refined using PRIME, IMP and **C64** were modeled and the overall structure was minimized. GLIDE (Schrödinger Inc.) was used to calculate a grid around **C64** with a single positional constraint on the carbon attached to the benzimidazole nitrogen. The grid was restricted to a size similar to **C64**. The inhibitor structures were converted to 3-D coordinates, pre-processed using ligprep to generate tautomers and ionization states at pH 2.0 – 7.0 and stored as sd files. GLIDE calculations were carried out in standard precision mode with the same single constraint. GLIDE automatically generated a pool of conformation for each inhibitor (~5000 each) and the best pose was chosen based on total number of productive interactions (both Van der Walls and electrostatic) with the protein. No water

molecules were included in this calculation. The structural overlay of the docked inhibitors showed < 1.5 Å deviation from **C64** indicating that GLIDE was able to reproduce the conformation of the inhibitors in the active site of CpIMPDH. For FEP calculations, DESMOND molecular dynamics engine (D.E Shaw Research and Schrödinger Inc.) with the OPLS2005 force field was used. In the current setup, a 22-window scheme was adopted for both A (WT) and B (B) states to achieve reasonably high accuracy. A simulation production time of 44 ns (2 ns × 22 windows) was used for all the calculations and the jobs were run on an in-house 24 node 3.4 GHz Beowulf cluster. Inhibitor **C** (IC_{50} = 1200 nM) was used as the initial structure (=0) to generate other structure in the series using alchemical FEP mutations.

14. Perkins ME, Wu TW, Le Blancq SM. Antimicrob Agents Chemother. 1998; 42:843. [PubMed: 9559794]
15. Woods KM, Nesterenko MV, Upton SJ. FEMS Microbiol Lett. 1995; 128:89. [PubMed: 7744242]
16. You X, Arrowood MJ, Lejkowski M, Xie L, Schinazi RF, Mead JR. FEMSMicrobiol Lett. 1996; 136:251.

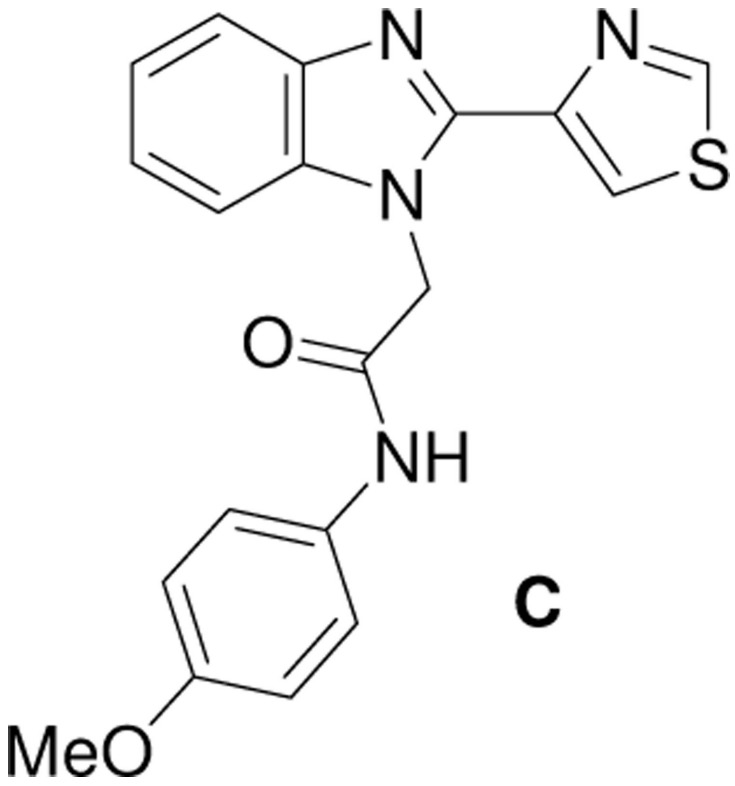

Figure 1.
*Cp*IMPDH selective inhibitor **C** identified by HTS

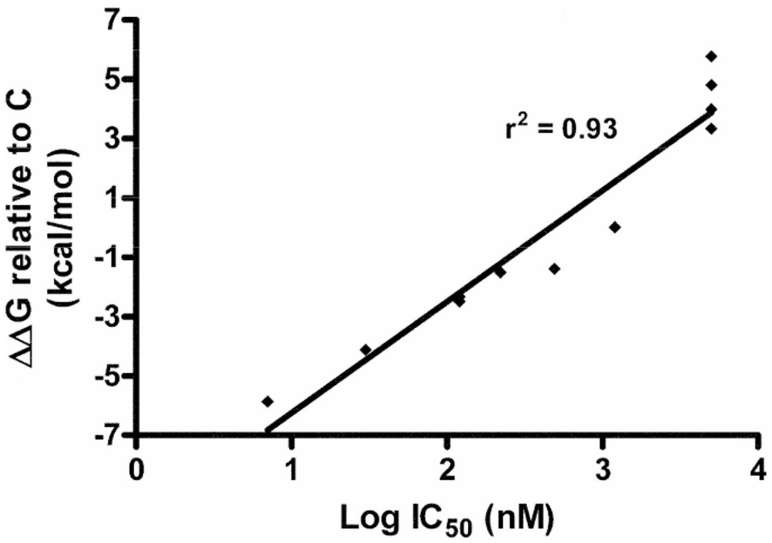

Figure 2.
Correlation of calculated relative affinity with experimental values.

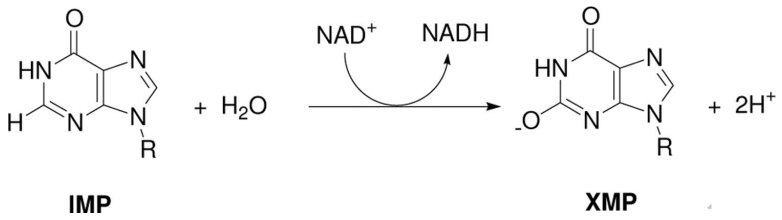

Scheme 1.
The IMPDH reaction. R = ribose-5'-phosphate

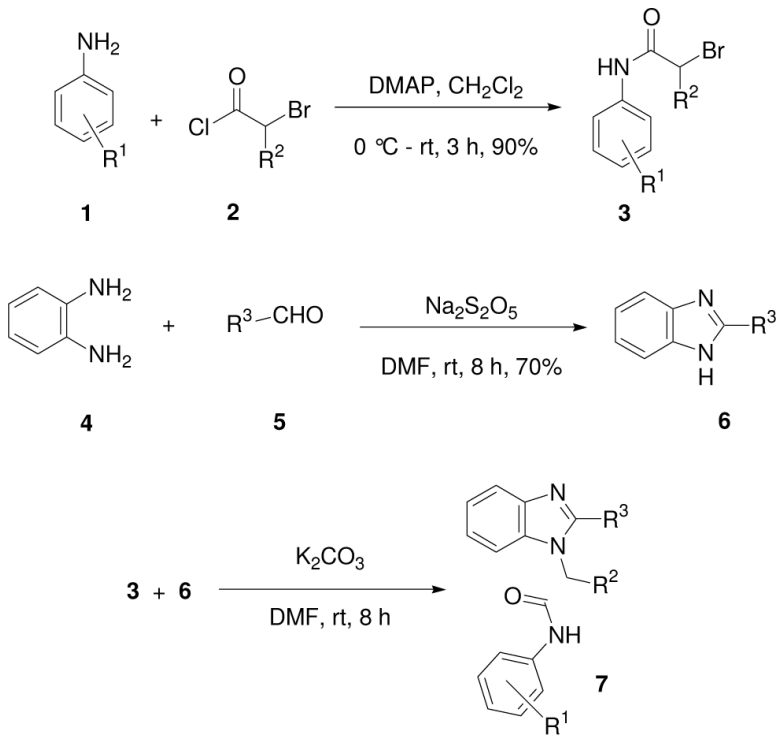

Scheme 2.
General procedure for synthesizing analogs of **C**.

Bioorg Med Chem Lett. Author manuscript; available in PMC 2013 March 01.

Table 1

SAR of the aniline ring.

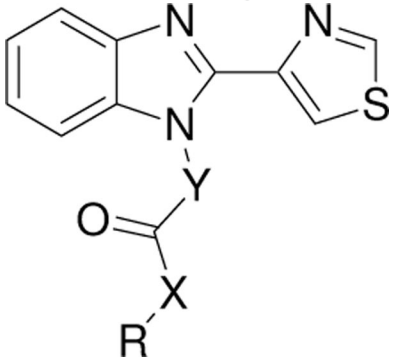

Compound	X	Y	R	IC_{50} (nM)	IC_{50} (nM) BSA
C [a]	NH	CH_2	4-OMePh	1200 ± 200	n.d.
C39	NH	CH_2	4-SMePh	120 ±40	69 ± 7
C43	NH	CH_2	4-*i*-PrPh	~ 5000	n.d.
C9	NH	CH_2	4-FPh	900 ± 100	n.d.
C10 [b]	NH	CH_2	4-ClPh	120 ± 40	200 ± 20
C11	NH	CH_2	4-CF_3Ph	220 ± 40	330 [d]
C58	NH	CH_2	4-CNPh	370 ± 60	n.d.
C14 [b]	NH	CH_2	4-BrPh	60 ± 30	n.d.
C40	NH	CH_2	4-SO_2MePh	~ 5000	n.d.
C45	NH	CH_2	4-OCF_3Ph	140 ± 50	n.d.
C20	NH	CH_2	2-ClPh	~ 5000	n.d.
C48	NH	CH_2	3-ClPh	490 ± 40	1430 [d]
C86 [b]	NH	CH_2	3,4-di-ClPh	30 ± 10	90 ± 2
C93	NH	CH_2	3-CN, 4-ClPh	30 ± 10	60 ± 20

Compound	X	Y	R	IC_{50} (nM)	IC_{50} (nM) BSA
C90 [b]	NH	CH_2	2-Naph	7 ± 4	20 ± 10
C28	NH	CH_2	1-(4-Cl)Naph	~ 5000	n.d.
C79	NH	$CH(CH_3)$	4-ClPh	60 ± 10	80 ± 20
C87	NH	$CH(CH_3)$	3,4-diClPh	240 ± 40	300 ± 70
C24	NH	CH(*i*Pr)	4-ClPh	~ 5000	n.d.
C18	CH_2NH	CH_2	4-ClPh	~ 5000	n.d.

All values are average of three independent determinations unless otherwise stated.

[a] data from 7;

[b] data from 10;

[c] n.d., not determined;

[d] n = 1;

Table 2

SAR of thiazole ring.

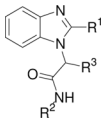

Compound	R^1	R^2	R^3	IC_{50} (nM)	IC_{50} (nM) BSA
C [a]	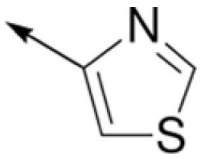	4-OMePh	H	1200	n.d.[c]
C61 [b]	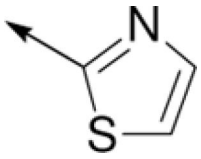	4-ClPh	H	30 ± 10	50 ± 10
C64 [b]		4-BrPh	H	28 ± 9	27[d]
C74		4-ClPh	Me	23 ± 4	30 ± 6
C84 [b]		3,4-diClPh	H	18 ± 5	50 ± 20
C97 [b]		2-Naph	H	8 ± 3	20 ± 20
C67	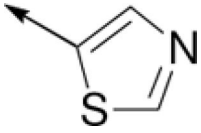	4-ClPh	H	35 ±9	60[d]
C62	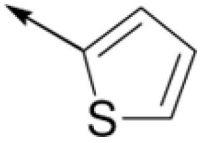	4-ClPh	H	20 ±20	60[d]

Compound	R^1	R^2	R^3	IC_{50} (nM)	IC_{50} (nM) BSA
C100	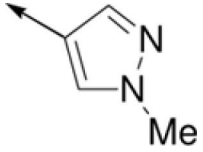	4-ClPh	H	35 ±8	42[d]
C16	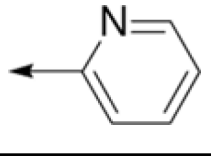	4-ClPh	H	43 ± 9	90 ± 30
C85		3,4-diClPh	H	22 ± 5	40 ± 7
C91		2-Naph	H	8 ± 3	14 ± 5
C92		3-CN, 4-ClPh	H	22 ± 10	40 ± 10
C65	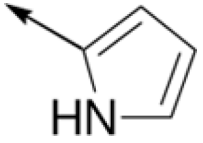	4-ClPh	H	80 ±10	120[d]
C69	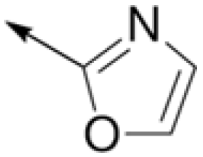	4-ClPh	H	170 ±10	230 ± 10
C17	Ph	4-ClPh	H	210 ±30	280 ± 30
C31	4-ClPh	4-ClPh	H	450 ± 20	n.d.
C59	4-FPh	4-ClPh	H	870 ± 20	1300[d]
C38	Me	4-ClPh	H	~5000	n.d.

All values are average of three independent determinations unless otherwise stated.

[a] data from[7];

[b] data from[10];

[c] n.d., not determined;

[d] n = 1;

Bioorg Med Chem Lett. Author manuscript; available in PMC 2013 March 01.

Table 3

Relative affinity of *Cp*IMPDH inhibitors based on docking experiments.[13]

Compound	ΔΔG relative to C (kcal/mol)
C	0
C39	−2.49
C43	4.8
C10	−2.34
C48	−1.39
C20	3.33
C86	−4.12
C90	−5.87
C40	3.99
C11	−1.51
C28	5.77

Table 4

Antiparasitic activity of selected compounds.

Compound	*T. gondii* model[a]			*C. parvum* model
	EC_{50}(μM)		Selectivity	
	Toxo/WT	Toxo/*Cp*IMPDH		EC_{50} (μM)
C64	>23	0.3 ± 0.1	>73	0.7 ± 0.2[c]
C84	3 ± 2	0.7 ± 0.3	5	1.7 ± 0.8[c]
C90	5 ± 1	0.6 ± 0.1	9	0.9 ± 0.5
C91	2.7 ± 0.9[c]	0.3 ± 0.2	9	n.d.
C97	17 ± 9	0.5 ± 0.4	30	< 0.8[d]

All values are the average of three independent trials unless otherwise stated.

[a] *T. gondii* model[12]. Toxo/WT, strain with endogenous IMPDH; Toxo/*Cp*IMPDH, strain that depends on *Cp*IMPDH. Selectivity = EC_{50}(Toxo/WT)/EC_{50}(Toxo/*Cp*IMPDH);

[b] *C. parvum* in vitro infection model;

[c] two determinations;

[d] Average growth inhibition 80 ± 10 % at 0.8 μM.